Kinetics and Mechanisms of Vinpocetine Degradation in Aqueous Solutions

NOUMAN MUHAMMAD, GLORIA ADAMS, AND HYUK-KOO LEE[x]

Received April 16, 1987, from *Pharmacy Research and Development, Ayerst Laboratories, Rouses Point, NY 12979.*
Accepted for publication September 10, 1987.

Abstract □ Under stressed conditions, vinpocetine (**1**; ethyl apovincamin-22-oate) equilibrates with vincaminic acid ethyl ester (**2**) and 14-epivincaminic acid ethyl ester (**3**), and hydrolyzes to apovincaminic acid (**4**). Sequentially, **2** is equilibrated with 14-epivincaminic acid ethyl ester (**3**) and hydrolyzes to vincaminic acid (**5**), which equilibrates with **4** and 14-epivincaminic acid (**6**). At acidic pH, the major route of degradation is **1** ⇌ **2** → **5**. However, at neutral pH, the major route of degradation is **1** → **4** ⇌ **5**. The kinetics for the degradation of **1** in the pH 1–3 region is represented by a consecutive reaction with a reversible step (second-order), but the degradation of **1** in the pH 3.5–6.0 region follows pseudo first-order kinetics. Significant buffer catalysis is observed with acetate and phosphate buffers. Reactions are dependent on the ionic strength, pH, and temperature. No oxygen effect on the degradation of vinpocetine is found.

Vinpocetine (ethyl apovincaminate-22-oate; AX-27,255) has been found to act as a cerebral vasodilator.[1] As a part of a vinpocetine preformulation study, this investigation was initiated to elucidate the degradation mechanism and to determine those kinetic parameters that will be of value in predicting the stability in aqueous solution. This will provide a basis for optimal design of appropriate dosage forms and a background for biopharmaceutical studies of the compound.

Experimental Section

Materials and Reagents—Vinpocetine (lot no. B42559A; ethyl apovincaminate-22-oate), manufactured by Gedeon Richter, Budapest, Hungary, was used. The reference standards,[2] apovincaminic acid (lot no. 800708), vincaminic acid ethyl ester (lot no. 800717-8), vincaminic acid (lot no. 850822), and vincamone (lot no. 800717-1), were also obtained from Gedeon Richter.

All solvents were spectro-grade and other chemicals were reagent grade.

High-Performance Liquid Chromatography Analysis—The HPLC system consisted of a Hewlett-Packard model 1082B LC with a 1040A detector (diode array detector), 7950B LC terminal, HP-85 PC, 82901 flexible disc drive, and 7470A plotter. This system possesses the capability of instant UV-VIS spectral scanning and storing-retrieving chromatographic data, with eight different signals monitored simultaneously.

The column used had an internal diameter of 150 × 4.6 mm and was packed with 5-μm SPHERISORB ODS reversed-phase materials. A flow rate of 1.5 mL/min was used for the mobile phase (30% acetonitrile and 70% 0.01 M monobasic potassium phosphate solution containing 0.01 M tetraethylammonium chloride and adjusted to pH 2.5 with phosphoric acid). A 50-μL injection volume was employed and the variable detector (1040A detector) was set at 280 nm.

A calibration standard was prepared each day from a stock solution of vinpocetine in methanol. The standard solution, containing 40, 50, or 60 μg/mL of vinpocetine, was prepared by appropriate dilutions with the mobile phase. After appropriate dilution of the samples with mobile phase solvent, samples were injected into the HPLC system by an auto sampler-injector. Each peak was computed automatically by the LC terminal. The column was flushed at the end of each day with water, followed by methanol.

Kinetic Procedures—A stock solution of vinpocetine (2.5 mg/mL) was prepared in methanol and stored in a low actinic volumetric flask. Aliquots were taken from the stock solution and diluted with the reaction media to produce a final concentration of 0.05 mg/mL in pH 1 to 5 buffer solutions and 0.03 mg/mL in pH 6.0 phosphate buffer solution. All sample solutions were purged with nitrogen in 2-mL amber glass ampules and then sealed.

Kinetic studies were carried out in constant-temperature oil baths or ovens at 70, 75, 80, and 85 °C. Samples were withdrawn at appropriate time intervals and subjected to HPLC analysis without dilution.

Oxidative Reaction in Solution—Sample solutions for oxidative reaction were prepared by the same procedures as for thermal reactive solutions. Each solution was placed in two amber glass ampules. One of each pair was purged with oxygen, the other was purged with nitrogen, and they were then sealed. The samples were placed in a constant-temperature oil bath at 80 °C. Aliquots were taken at appropriate time intervals and directly subjected to HPLC analysis.

Metal Ion Analysis—Metal ion analysis was done by Spectra Co. (San Diego, CA) using emission spectroscopy (ASTM Method No. E-2-SM-11-22).

Results and Discussion

Identification of Degradation Products—A typical HPLC scan for the degradation reaction in 0.1 M HCl at 80 °C for 14 d (in ampule) and the on-line UV spectrum of each degradation product peak is shown in Figure 1.

Peaks were tentatively identified based on comparison of retention time and on-line UV spectra with the authentic compounds:[2] peak 1 (RT 12 min) as vinpocetine (**1**), peak 2 (RT 4.3 min) as vincaminic acid ethyl ester (**2**), peak 4 (RT 1.5 min) as apovincaminic acid (**4**), peak 5 (RT 1.0 min) as vincaminic acid (**5**), and peak 7 (RT 2.9 min) as vincamone (**7**).

Peaks 3 (RT 3.8 min) and 6 (RT 0.99 min) were not directly compared with 14-epimers of products 2 and 5 due to unavailability of the authentic compounds. However, peaks 3 and 6 are tentatively assigned as 14-epivincaminic acid ethyl ester (**3**) and 14-epivincaminic acid (**6**), respectively, since the UV spectrum of peaks 3 and 6 is almost identical to that of peaks 2 and 5, and the retention times of peaks 2 and 3, and 5 and 6 are close to each other.

Other unidentified minor peaks at retention times of 5.0, 2.30, and 1.93 min were found at <1% formation in 0.1 M HCl at 80 °C for 32 d. No further attempt was made to identify these minor products. The general degradation scheme is depicted in Scheme I.

Reaction Order and Rate Constants—Typical semilogarithmic plots for the percent of vinpocetine remaining versus time at pH 2 and 5 at 85 °C are shown in Figure 2. These plots for the pH 1–3 region exhibit a biphasic curve indicating that the kinetics are consecutive reactions with a reversible step (second-order kinetics): the reversible process (2 ⇌ 1) was confirmed by independent kinetic study of 2 in 0.1 M HCl at 85 °C; the initial reactant 2 was transformed to give products 1, 3, and 5. However, the plot for the pH 3.5–7.0

0022-3549/88/0200-0126$01.00/0

region gives a straight line ($r \simeq 0.99$), and indicates that the reactions follow pseudo first-order kinetics at constant pH and temperature conditions. In this region, the reversible step (k_{21}) may not be a significant contribution to the reaction.

In the acidic region of pH 1–3, the initial rate method was used to get the first-order rate constant (k_{app}). The chief practical advantage of this method is the saving of time needed to construct the logarithmic apparent first-order rate (k_{app})–pH profile for the entire pH range. The disadvantage is overestimation of the actual rate by neglecting the reverse reaction.

Effect of Buffer Concentrations—The apparent first-order rate constant (k_{app}) in a buffer solution is the sum of catalytic contributions from the hydrogen ion, the hydroxide ion, and the acidic (HA) and basic (A) components of a buffer and water species. The overall rate constants for reaction in a buffer may be expressed by:[3]

$$k_{app} = k_o + k_{H^+}[H^+] + k_{HA}[HA] + k_{A^-}[A^-] + k_{OH^-}[OH^-] \quad (1)$$

or:

$$k_{app} = k_0 + \left(k_{HA} + \frac{k_A K_a}{[H^+]}\right)[HA] + k_{H^+}[H^+] + k_{OH^-}[OH^-] \quad (2)$$

or:

$$k_{app} = k_0 + k_{H^+}[H^+] + k_{OH^-}[OH^-] + \left(k_{A^-} + \frac{k_{HA}[H^+]}{K_a}\right)[A^-] \quad (3)$$

Thus, a plot of k_{app} versus [HA] at a constant pH will be linear with an intercept of ($k_o + k_{H^+}[H^+] + k_{OH}[OH^-]$), and a slope of $S_1 = k_{HA} + k_{A^-}K_a/[H^+]$. A plot of k_{app} versus $[A^-]$ at a constant pH will give a straight line with an intercept of ($k_o + k_{H^+}[H^+] + k_{OH}[OH^-]$) and a slope of $S_2 = k_{A^-} + k_{HA}[H^+]/K_a$. A plot of k_{app} versus [HA], or k_{app} versus $[A^-]$, at two or more pH values, will permit the calculation of both catalytic constants, k_{HA} and k_{A^-}.

Significant buffer catalysis was observed with acetate and phosphate buffers. Apparent first-order rate constants were measured as a function of buffer concentration and temperature. From the plots of k_{app} versus [HAc] and [Ac], the respective slopes of $S_1 = k_{HAc} + k_{Ac}K_a/[H^+]$ and $S_2 = k_{Ac} + k_{HA}[H^+]/K_a$ were obtained and are listed in Table I.

Effect of Ionic Strength—An investigation of the disappearance rate of vinpocetine as a function of ionic strength was carried out to determine the influence of electrolytes. To conduct these studies, solutions were prepared at constant pH 1.1 (0.1 M HCl) and pH 6.0 ± 0.05 (phosphate buffer, 0.1 M) at 75 °C, with varying ionic strength. The ionic strength was varied by adding sodium chloride.

The relationship between the rate constant and ionic strength (μ) is given by the Bronsted–Bjerrum equation.[4]

$$\ln k_{app} = \ln k_o + 2QZ_AZ_B\sqrt{\mu} \quad (4)$$

where k_o is the rate constant in an infinitely dilute solution at $\mu = 0$, Z_A and Z_B are the charge on reaction species A and B, respectively, and Q is a constant at given temperature ($Q = 0.5115 \times 2.303$ at 25 °C, $Q = 0.5695 \times 2.303$ at 75 °C).[5] Plots based on this equation should yield a linear relationship with a slope proportional to the product of the charge carried by the reactive species forming the activated complex.

Semilogarithmic plots of the k_{app} versus the square root of ionic strength ($\sqrt{\mu}$) resulted in a straight line ($r = 0.99$), indicating that the reactions were dependent on the ionic strength. The slope of the regression line fitted data was close to positive unity at pH 1.1 and negative unity at pH 6.0. The results justified a specific acid and specific base catalysis on the positively charged species of vinpocetine.

pH Dependency—The pH dependency of k_{app} for the disappearance of vinpocetine as a function of pH and temperature at constant ionic strength of 0.1 is shown in Figure 3. The rate used in the construction of the rate–pH profiles (Figure 3) was obtained from the initial rate method at pH 1–3 and from the intercepts of the plots of k_{app} versus buffer concentration at pH 3.5–6.0. Unfortunately, the k_{app} values at pH values >6 could not be obtained due to low solubility.

In the rate–pH profile, the k_{app} at pH values <3.0 decreases linearly with increasing pH, with a slope of about unity. This suggests that a specific acid-catalyzed reaction is important: a reduction of the fraction of protonated species attacked by neutral water molecules is kinetically equivalent to a hydrogen ion attack on the neutral substrate. The plateau portion at pH 3.5 to 4.0 suggests that water attack on the protonated species is significant. The k_{app} values at pH values >4.0 increased with increasing pH; hydroxide ion attack on the protonated species is kinetically equivalent to water attack on the neutral species. The profile inflection near pH 6.0 indicates that k_{app} may be influenced by the K_a value.

Thus, the profiles at the pH 1–6 region were fitted to:

$$k_{app} = \left(k_0 + k_{H^-}[H^+] + k_{OH^-}\frac{K_w}{[H^+]}\right)\frac{[H^+]}{[H^+] + K_a} \quad (5)$$

where k_o is the first-order rate constant for neutral water catalysis, k_{H^+} and k_{OH^-} are the second-order rate constants for specific hydrogen ion and hydroxide ion catalyses, respectively, K_w is the water dissociation constant, and K_a is the

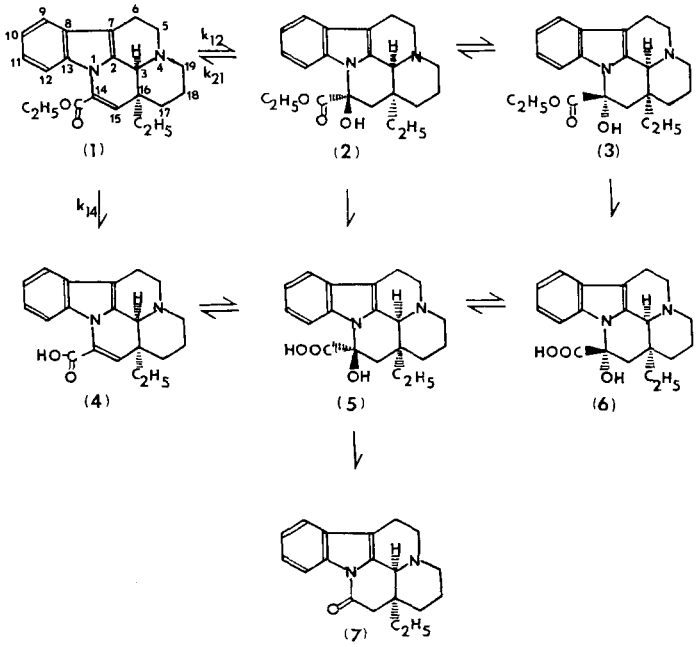

Scheme I

dissociation constant of vinpocetine.

The k_o, k_{H^+}, k_{OH^-}, and K_a values were estimated from the best fit of the rate–pH profiles and the results are shown in Table II. The theoretical degradation rates were calculated at the pH 1–6 range by employing the K_w value at the given temperature. The K_w value was obtained or extrapolated from literature data:[5] 3.090×10^{-13} at 85 °C; 2.500×10^{-13} at 80 °C; 2.005×10^{-13} at 75 °C; and 1.585×10^{-13} at 70 °C.

In Figure 3 the line represents the theoretical curve calculated by substituting the microscopic constants into eq 5, while the points show the experimental results. The good agreement indicates that eq 5 adequately describes the

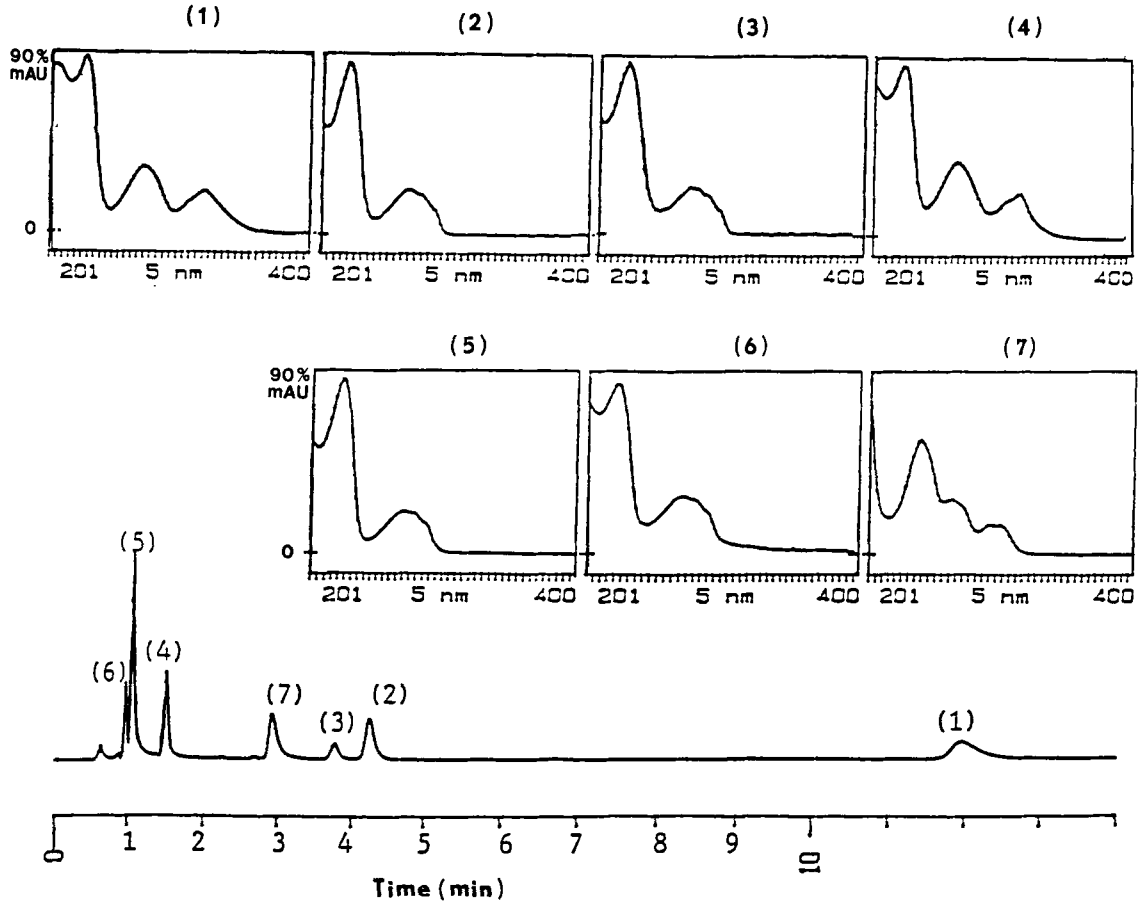

Figure 1—*Typical HPLC scan for the degradation of vinpocetine in 0.1 M HCl at 80 °C for 14 d and on-line UV spectrum of each product (in ampule). Key:* (**1**) *vinpocetine (RT = 12);* (**2**) *vincaminic acid ethyl ester (RT = 4.3);* (**3**) *14-epivincaminic ethyl ester (RT = 3.8);* (**4**) *apovincaminic acid (RT = 1.5);* (**5**) *vincaminic acid (RT = 1.0);* (**6**) *14-epivincaminic acid (RT = 0.99);* (**7**) *vincamone (RT = 2.9).*

Table I—Data for Acetate Buffer Catalysis at Various pH Values and Temperatures[a]

	$1/[H^+]$ versus $S_1 = k_{HA} + k_{A^-} K_a/[H^+]$				
pH	$1/[H^+]$	85 °C S_1	80 °C S_1	75 °C S_1	70 °C S_1
4.0	1×10^4	3.22×10^{-7}	1.89×10^{-7}	1.33×10^{-7}	9.95×10^{-8}
4.5	3.162×10^4	6.94×10^{-7}	4.08×10^{-7}	2.67×10^{-7}	1.82×10^{-7}
5.0	1×10^5	1.46×10^{-6}	7.95×10^{-7}	7.27×10^{-7}	4.82×10^{-7}
5.5	3.162×10^5	3.79×10^{-6}	—	1.68×10^{-6}	1.31×10^{-6}
	k_{HA} ($M^{-1} \cdot s^{-1}$)	$(2.94 \pm 0.55) \times 10^{-7}$	$(1.58 \pm 0.53) \times 10^{-7}$	$(1.32 \pm 0.56) \times 10^{-7}$	$(6.65 \pm 1.23) \times 10^{-8}$
	$[H^+]$ versus $S_2 = k_{A^-} + k_{HA} [H^+]/K_a$				
pH	$[H^+]$	85 °C S_2	80 °C S_2	75 °C S_2	70 °C S_2
4.0	1×10^{-4}	1.83×10^{-6}	1.08×10^{-6}	7.59×10^{-7}	5.67×10^{-7}
4.5	3.162×10^{-5}	1.25×10^{-6}	7.36×10^{-7}	4.78×10^{-7}	3.26×10^{-7}
5.0	1×10^{-5}	8.33×10^{-7}	4.49×10^{-7}	4.11×10^{-7}	2.75×10^{-7}
5.5	3.162×10^{-6}	6.83×10^{-7}	—	3.43×10^{-7}	2.36×10^{-7}
	k_{A^-} ($M^{-1} \cdot s^{-1}$)	$(7.38 \pm 0.90) \times 10^{-7}$	$(4.47 \pm 0.97) \times 10^{-7}$	$(3.49 \pm 0.14) \times 10^{-7}$	$(2.30 \pm 0.08) \times 10^{-7}$

[a] Expressed as estimate ± SD.

kinetics of vinpocetine degradation.

Temperature Dependency—Estimates of the Arrhenius parameters for the degradation of vinpocetine are obtained from the slopes and intercepts of plots of log k_{app} versus the reciprocal of the absolute temperature (T), in accordance with eq 6:

$$\ln k_{app} = \ln A - E_a/RT \quad (6)$$

where A is the frequency factor, E_a is the activation energy, and R is the gas constant (1.987 cal/deg·mol). The entropy of activation, $\Delta S^{\ddagger}$, is calculated from the ln A values using eq 8:[4]

$$A = (kT/h)e^{(\Delta S^{\ddagger}/R)} + 1 \quad (7)$$

and then,

$$\Delta S^{\ddagger} = R(\ln A - \ln kT/h - 1) \quad (8)$$

where k is the Boltzmann constant (1.381×10^{-16} erg/deg) and h is the Planck constant (6.625×10^{-27} erg·s).

The obtained Arrhenius parameters are shown in Table II. Activation energies of 10 to 15 kcal/mol are observed. The observed large negative entropy of activation ($\Delta S^{\ddagger}$) suggests that a bimolecular reaction is involved at the transition state.

The k_o value at 25 °C can be estimated from the Arrhenius

Table II—Microscopic Constants[a] and Arrhenius Parameters for Degradation of Vinpocetine

Temperature (t), °C	k_{H^+} (M^{-1}, S^{-1})	k_o (S^{-1})	k_{OH} (M^{-1}, S^{-1})	K_a
85	5.399×10^{-5}	2.363×10^{-8}	4.156	9.327×10^{-7}
80	3.948×10^{-5}	1.700×10^{-8}	3.022	7.965×10^{-7}
75	2.954×10^{-5}	1.279×10^{-8}	2.179	6.521×10^{-7}
70	1.967×10^{-5}	9.205×10^{-9}	1.565	4.880×10^{-7}
25	5.561×10^{-7}[b]	3.181×10^{-10}[b]	4.618×10^{-2}[b]	6.064×10^{-8}
ln A	12.97 ± 1.08	3.78 ± 0.48	23.77 ± 0.07	−0.24 ± 0.26
E_a, kcal/mol	16.21 ± 0.75	15.19 ± 0.34	15.89 ± 0.05	9.701 ± 0.18
$\Delta S^{\ddagger}$ at 25 °C, eu	−34.75 ± 2.14	−53.00 ± 0.96	−13.30 ± 0.15	−61.00 ± 0.53

[a] Expressed as estimate ± SD; based on the kinetic expression for degradation of vinpocetine (eq 5), where K_w values used are 3.090×10^{-13} at 85 °C, 2.500×10^{-13} at 80 °C, 2.005×10^{-13} at 70 °C, and 1.585×10^{-13} at 70 °C; those values are obtained or extrapolated for the requisite temperature from ref 5. [b] The microscopic rate constants at 25 °C were estimated from the Arrhenius equation (eq 6).

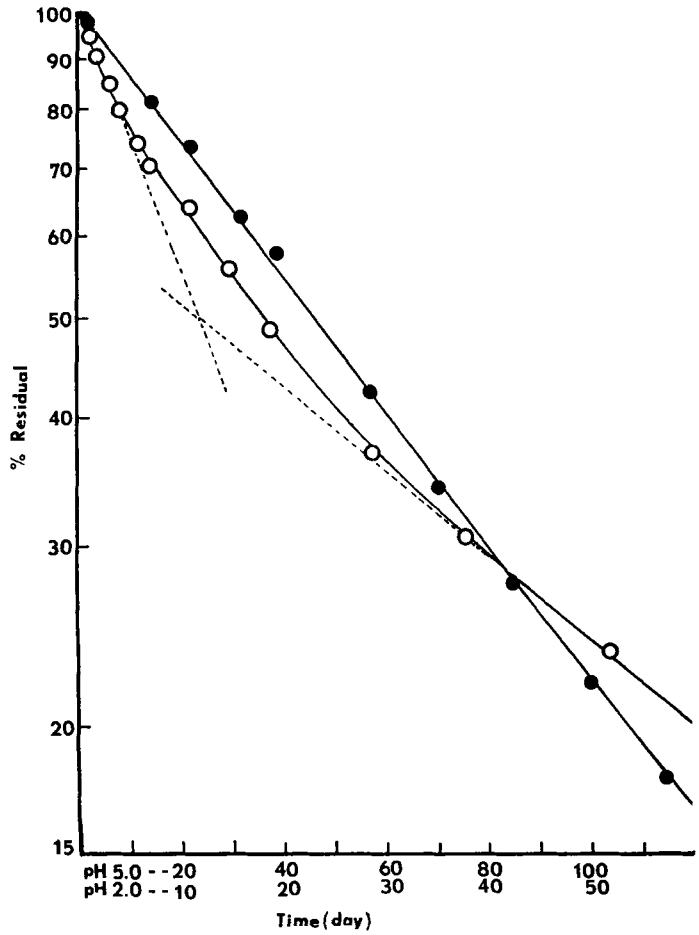

Figure 2—*Typical semilog plots for disappearance of vinpocetine versus time at pH 2 and 5, at 80 °C. Key: (○) pH = 2.0; (●) pH = 5.0.*

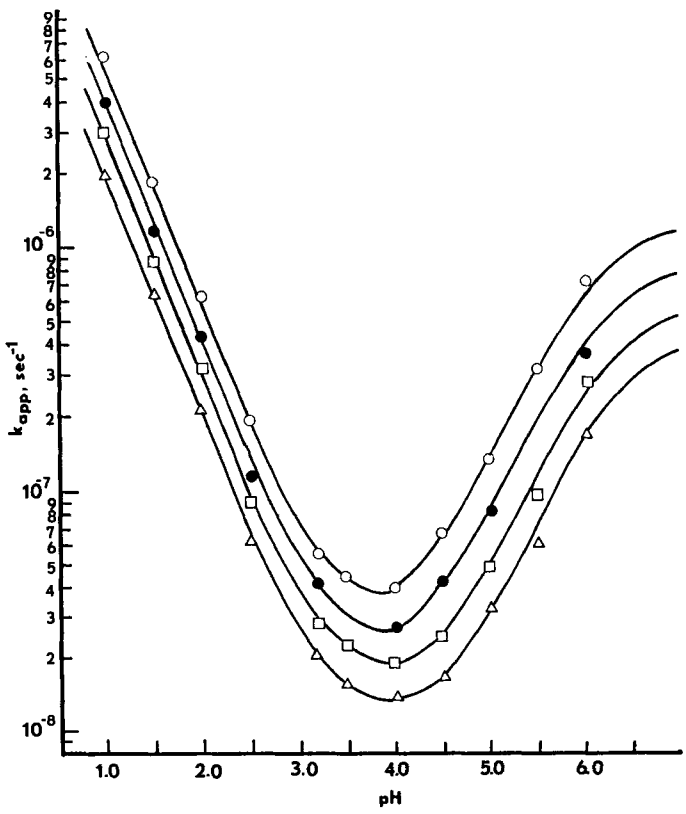

Figure 3—*Logarithmic k_{app}–pH profile for the disappearance of vinpocetine at various pH values and temperatures, and at constant ionic strength of 0.1. Key: (○) 85 °C; (●) 80 °C; (□) 75 °C; (△) 70 °C.*

equation as listed in Table II. At the most stable region (pH 3.5–4.0), the time required for 3% degradation (t_{97}) in aqueous solution is estimated as 3 years.

Oxygen Effect—The 0.1 M HCl solution of vinpocetine purged with nitrogen and oxygen was studied at 80 °C. The disappearance rate of vinpocetine with oxygen was not significantly different from that with nitrogen. However, the rate of vincamone (**5**) formation from vinpocetine purged with oxygen was significantly faster than that from vinpocetine purged with nitrogen in the ampule. The results suggest that free acid forms of the compound, **4**, **5**, or **6**, can be oxidized, but not the ester forms, **1**, **2**, and **3**.

Degradation Mechanism—Typical concentration–time profiles for the degradation of vinpocetine and the formation of degradation products in pH 5.5 phosphate buffer at 80 °C and 0.1 M HCl at 80 °C are presented in Figures 4 and 5, respectively.

As shown in Figure 6, vinpocetine (**1**) at acidic pH is transformed to hydrated products **2** and **3** through the enamine-type intermediates, **1a** and **1b**.[6] Due to the electron-withdrawing effect of the double bond between C_{14} and C_{15} and electron delocalization of the nitrogen lone pair, *N*-protonated enamine (enammonium ion, **1a**) in acidic solution may be kinetically favored, and it is slowly converted to the thermodynamically more stable C_{15}-protonated enamine (iminum ion, **1b**). Then, more stable iminum ion (**1b**) can be susceptible to water attack to form either **2** or **3** (Scheme II).

The equilibrium constant of **2** with **3** ($K_e = [3]_e/[2]_e$) in 0.1 M HCl at 85 °C was found to be 0.3, indicating that the formation of **2** (equatorial position of the ester group) is more favorable (~3 times) than that of **3** (axial position of the ester group). Vinpocetine also is hydrolyzed to give apovincaminic acid (**4**; Figures 4–6). Products **2** and **3** also are hydrolyzed to form products **5** and **6**, respectively. These transformations were confirmed by independent kinetic studies of **2**, **4**, and **5** conducted in 0.1 M HCl at 85 °C. Initial reactant **2** was transformed to give products **1**, **3**, and **5**. Then, product **1** was sequentially hydrolyzed to yield product **4**. Product **5** from **4** and **4** from **5** were also obtained, respectively. These results indicate that equilibrium reactions between **1** and **2**, **2** and **3**, and **4** and **5**, respectively, can occur. In an analogous manner to Scheme II, product **5** can be formed from **4** (via enammonium and iminum ion-type intermediate) by hydration and from **2** by hydrolysis.

An unusual observation was made on the reaction in the volumetric flasks (Pyrex glass) when compared with the reaction in ampules (soda glass). At acidic pH, the thermodynamically stable oxidation product vincamone (**7**) was formed from the reaction in sealed ampules (Figure 6). When all sample solutions were purged with nitrogen in 2-mL amber glass ampules and sealed, the formation of **7** decreased with increasing pH over the range 1–3. However, when the kinetic study in 0.1 M HCl at 80 °C was conducted in the 50-mL low actinic volumetric flask that was purged with nitrogen, no significant amount of **7** was found (Figure 5). In both cases, no variation in rate of vinpocetine disappearance was observed. This information coupled with no oxygen effect on vinpocetine disappearance and significant oxygen effect on the formation of **7** indicates the free acid form, **4**, **5**, or **6**, may be oxidized to give the oxidized product **7**. However, decar-

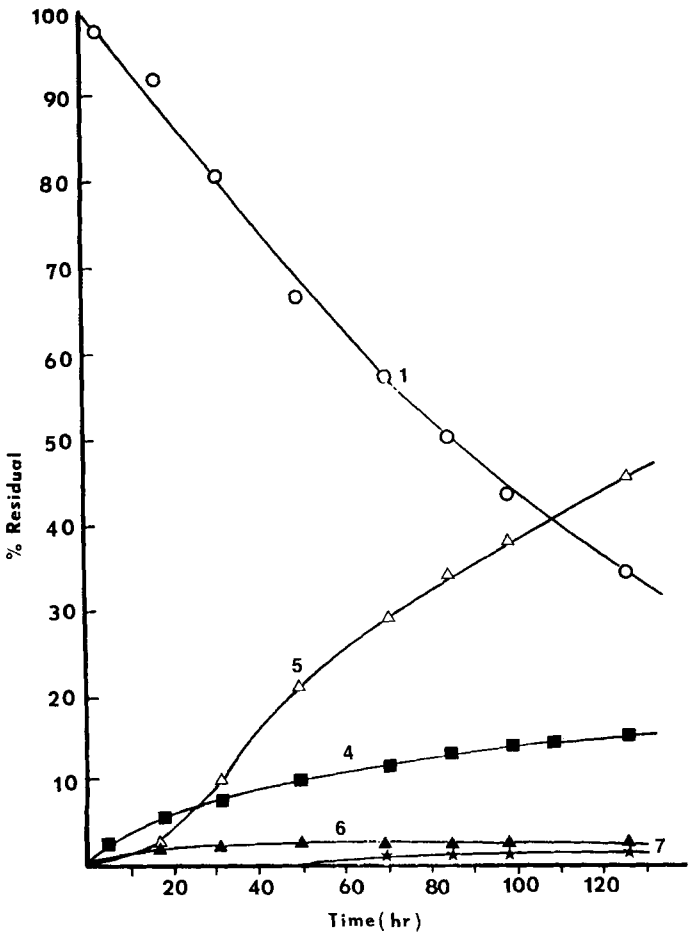

Figure 4—*Degradation profile of vinpocetine at pH 5.5 and 80 °C (in ampule). Key:* (○) *vinpocetine* (**1**); (■) *apovincaminic acid* (**4**); (△) *vincaminic acid* (**5**); (▲) *14-epivincaminic acid* (**6**); (★) *vincamone* (**7**).

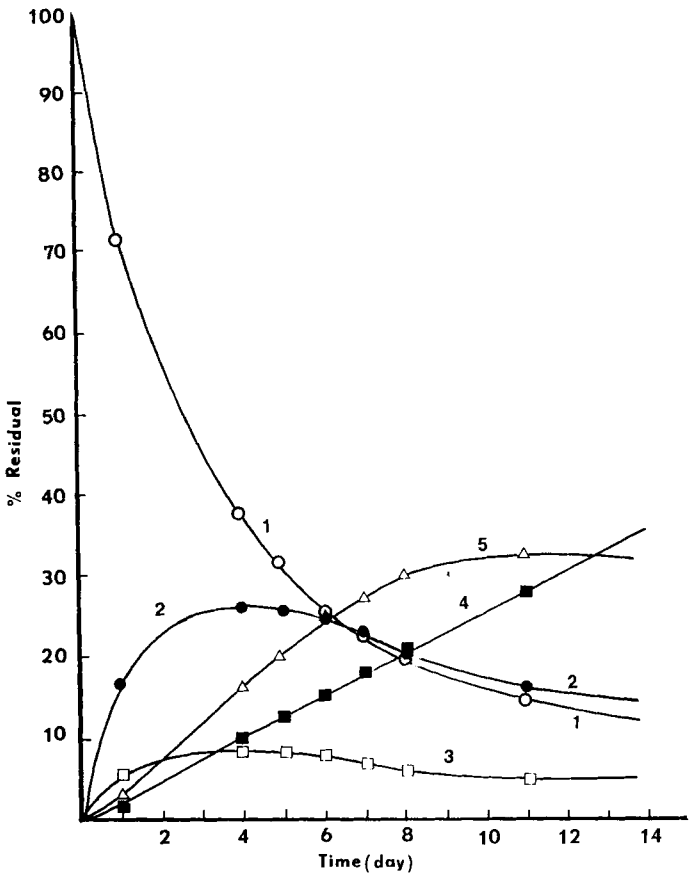

Figure 5—*Vinpocetine degradation profile in 0.1 M HCl at 80 °C (in Pyrex flask). Key:* (○) *vinpocetine* (**1**); (●) *vincaminic acid ethyl ester* (**2**); (□) *14-epivincaminic acid ethyl ester* (**3**); (■) *apovincaminic acid* (**4**); (△) *vincaminic acid* (**5**).

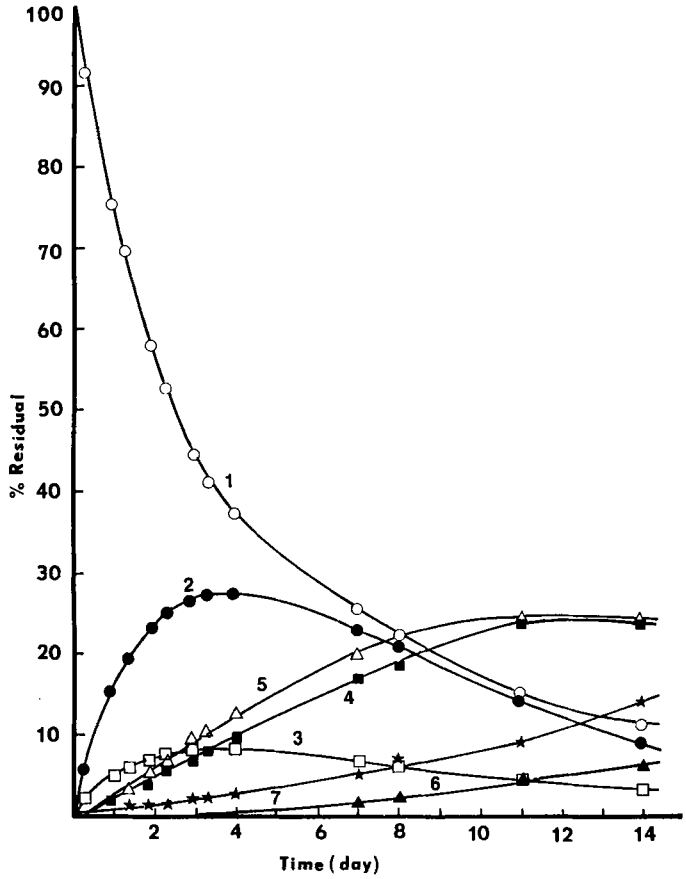

Figure 6—*Degradation profile of vinpocetine in 0.1 M HCl at 85 °C (in ampule). Key:* (○) *vinpocetine* (**1**); (●) *vincaminic acid ethyl ester* (**2**); (□) *14-epivincaminic acid ethyl ester* (**3**); (■) *apovincaminic acid* (**4**); (△) *vincaminic acid* (**5**); (▲) *14-epivincaminic acid* (**6**); (★) *vincamone* (**7**).

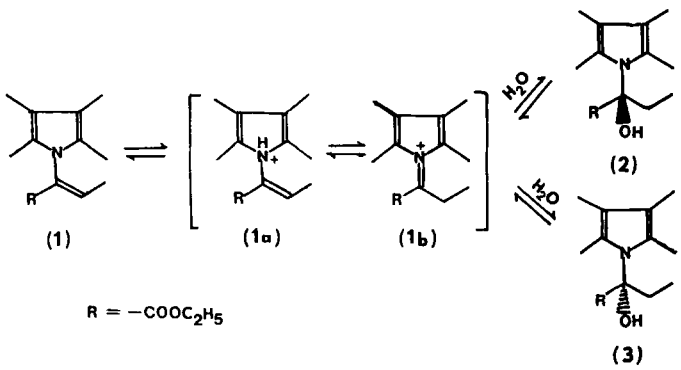

Scheme II

boxylation of the ester forms 1, 2, and 3 is very unlikely to occur.[7]

Metal ion analysis of the 0.1 M HCl sample solution in an ampule at 80 °C for 6 d showed that no significant amount (<5 ppm level) of heavy metals was present in solution to catalyze the reaction, except >100 ppm of sodium was found. However, this finding cannot rule out the effect of heavy metal ions on the surface of the ampule container. The analogous reaction has been reported in the case of tryptophan autoxidation in aqueous HCl at 100 °C; impurities present in the soda glass containers used were responsible for the initiation of the reaction.[8] Thus, for the formation of 7 from 5, heavy metal ions on the soda glass surface may catalyze the reaction. Although intimate details for the decarboxylation mechanism of the free acid are not clearly understood, Brower et al.[9] argue that the Zwitterion mechanism is in better agreement with data from the effect of solvent on the volumes of activation: the Zwitterion mechanism appears attractive for picolinic and related acids. The effect of various metal ions on the rate of acid decarboxylation was explored: metal ions catalyze the decomposition of oxalacetic[10] and dimethyl oxalacetic[11] acids. During the catalyzed decarboxylation, a metal ion complex of the di-ion is probably formed.

From the above information, one may reasonably speculate the oxidative decarboxylation mechanism for the transformation of 5 from 7 shown in Schemes III or IV. All the evidence so far cited by Pocker and Davis[12] indicates that 2-hydroxycarboxylic acid oxidations occur via a more or less concerted mechanism in which the rate-determining step involves the decomposition of a metal-hydroxy acid intermediate. On the basis of the study by Pocker and Davis,[12] it seems more probable that cyclic intermediate **5c** or **5d** is involved in the rate-determining step in Schemes III and IV.

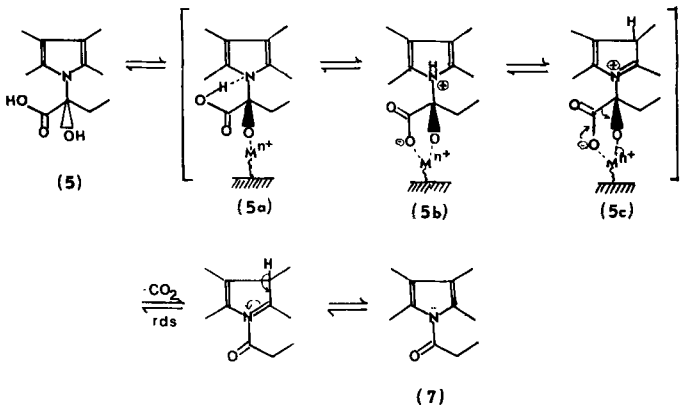

Scheme III

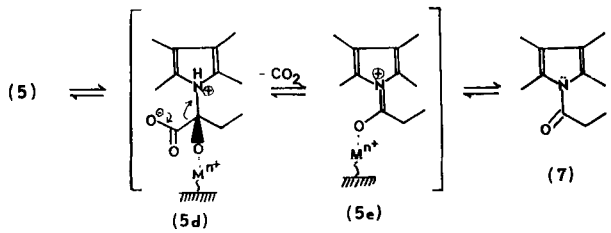

Scheme IV

References and Notes

1. Orosz, E.; Deak, G.; Benoist, G. *Arzneim.-Forsch.* **1976**, *26*, 1951.
2. Szepesi, G.; Gazdag, M. *J. Chromatogr.* **1981**, *204*, 341.
3. Garrett, E. R. In *Advances in Pharmaceutical Sciences*, Vol. II; Academic: New York, NY, 1967; pp 1–94.
4. Frost, A.; Pearson, P. *Kinetics and Mechanisms*, 2nd ed.; Wiley: New York, NY, 1962; pp 101, 150.
5. Robinson, R. A.; Stockes, R. H. *The Electrolyte Solutions*, 2nd ed.; Butterworths: London, 1959; p 468.
6. Hickmott, P. W. *Tetrahedron* **1982**, *38 (14)*, 1975.
7. Steinberger, R.; Westheimer, F. *J. Am. Chem. Soc.* **1949**, *71*, 4158.
8. Stewart, M.; Nicholls, C. H. *Aust. J. Chem.* **1972**, *25*, 2139.
9. Brower, K. R.; Gay, B.; Konkol, T. L. *J. Am. Chem. Soc.* **1966**, *88*, 1681.
10. Tsai, C. S. *Can. J. Chem.* **1967**, *45*, 873.
11. Steinberger, R.; Westheimer, F. H. *J. Am. Chem. Soc.* **1951**, *73*, 429.
12. Pocker, Y.; Davis, B. C. *J. Am. Chem. Soc.* **1973**, *95*, 6216.

Acknowledgments

The authors wish to thank Dr. Ivo Jirkovsky for helpful discussions.